ADSORPTION OF ATRAZINE IN RICE HUSK BIOCHARS: A PHENOMENOLOGICAL MODEL APPLIED TO EQUILIBRIUM AND KINETIC STUDIES

Juliana Luconi[1*], Mariana Sbizzaro[1], Cleuciane T. do Nascimento[2], Silvio C. Sampaio[1], Ralpho R. dos Reis[1]

[1*]Corresponding author. UNIOESTE/ Cascavel - PR, Brasil.
E-mail: julianaluconi@hotmail.com | ORCID ID: https://orcid.org/0000-0001-7769-0079

KEYWORDS

biochar, mathematical
modeling,
intraparticle diffusion.

ABSTRACT

Atrazine is an herbicide used to remove weeds in agricultural crops; however, because it is considered toxic, options for removing it from the environment are needed. Adsorption on biochar is an efficient technique for removing organic contaminants. In this study, the atrazine adsorption capacities of two biochars (BCA400 and BCA700) produced from rice husks at different pyrolysis temperatures (400 and 700 °C) were compared by phenomenological modeling. The biochars were characterized by SEM, FTIR and BET. Experimental kinetic and equilibrium data were obtained to evaluate Langmuir, Freundlich and BET isotherms and to conduct intraparticle diffusion. In comparison to BCA400, BCA700 showed a higher adsorption capacity at a higher pyrolysis temperature, and the Freundlich isotherm best described its system. To describe the kinetic adsorption data for the biochars, a phenomenological model based on intraparticle diffusion was applied, and the model fit well to these data for each biochar. This model is slow and involves the transport of atrazine to the pores of the biochar. Thus, the predictive model can be scaled up to adsorption systems.

INTRODUCTION

Atrazine is one of the most commonly used agricultural herbicides and is effective in preventing weeds, predominantly in corn, sorghum, and sugarcane crops (Tao et al., 2020). It is considered toxic to aquatic organisms, plants, and humans because it is moderately mobile and has a long half-life, high leaching potential and high chemical stability (Zhang et al., 2018; Gao et al., 2019). Thus, techniques to remove atrazine are necessary to meet environmental quality requirements. Conventional removal methods have some undesirable characteristics, such as high costs and low efficiency levels (Mohan et al., 2014).

Biochar adsorption is a method that has been used to remove atrazine because it addresses these negative aspects because it is highly efficient, easy to apply, and inexpensive (Yang et al., 2018; Zhang et al., 2018). Biochar adsorption also provides an adequate destination for plant residues, which are used as raw materials. In addition,

several studies (Yang et al., 2017; Ren et al., 2018; Suo et al., 2019; Gao et al., 2019) have demonstrated the use of biochars as effective adsorbents in the removal of various organic contaminants in water.

Rice husk is considered a biochar that is produced in a sustainable manner and that can be an alternative to the traditional use of other biochar types, such as wood (BUDEMBERG, 2013). Rice husks represent approximately 20% of rice mass, and when discarded, their high volume and slow natural absorption in the environment cause concern (Abdulrazzaq et al., 2014). Previous studies have shown that the use of rice husk biochar is efficient in removing contaminants in an aqueous medium (Lingamdinne et al., 2015; Kizito et al., 2015; Vithanage et al., 2016; Chen et al., 2019). The efficiency of pesticide removal by biochars in aqueous solutions depends on their raw material source, the pyrolysis conditions, and their physical and chemical properties (Usman et al., 2016; Yang

et al., 2018). Such characteristics include high specific surface area, porosity, polyaromatic structure, and diversity of functional groups (Liang et al., 2017; Zhang et al., 2018).

The use of a mathematical model is essential for researching and developing various processes, including adsorption. Modeling aims to optimize the operational conditions of a process and understand the physical and chemical mechanisms involved in the process. Phenomenological models are recommended for describing equilibrium and kinetic adsorption, leading to a more conclusive understanding because they are more predictive than empirical models and reveal physically significant kinetic parameters. The classic models (pseudo first order and pseudo second order), although representative and widespread, are not as capable of demonstrating a definitive process (Monte Blanco et al., 2017).

The importance of developing research to understand the benefits of using biochar as a contaminant adsorbent is clear, with the goal of using new, low-cost adsorbents in the removal and/or reduction of pesticides in waters and soils. Thus, the present study aims to evaluate the adsorption capacity of two biochars obtained from rice husks for the herbicide atrazine through phenomenological modeling.

MATERIAL AND METHODS

The biochars used in the present study were produced and provided by Embrapa Floresta, located in the municipality of Colombo, PR. The materials were produced from rice husk, which was dried in an oven at 110 °C for 24 hours. The pyrolysis was performed in a muffle furnace under a low oxygen concentration for one hour at temperatures of 400 °C and 700 °C, with a heating rate of 10 °C min^{-1}. Both samples were ground and sieved through a 0.075 mm mesh to standardize the particle size, according to the methodology proposed by Zheng et al. (2010). The samples were named according to the pyrolysis temperature (BCA400 and BCA700).

The biochars were characterized by scanning electron microscopy (SEM), Fourier transform infrared spectroscopy (FTIR), and the Brunauer–Emmett–Teller (BET) method.

The herbicide used in the study, atrazine ($C_8H_{14}ClN_5$), was purchased from Sigma–Aldrich Corporation, and was 99% pure. From this, a stock solution of 500 mg L^{-1} in methanol was prepared. The determination of atrazine concentration was performed by high-performance liquid chromatography (HPLC) using a Shimadzu® Prominence Chromatograph.

Kinetic study

The adsorption kinetic tests were performed in batches to determine the equilibrium time and the kinetic model that controlled the process. All experimental treatments were performed in triplicate. In each assay, 20 mg of biochar was placed in a glass tube, and then, 10 mL of the atrazine solution at a concentration of 10 mg L^{-1} was added. The samples were placed in a shaker with a controlled temperature of 22 ± 0.5 °C at 180 rpm.

The kinetic test continued for 480 hours, and the flasks were removed from the shaker at predefined times (3, 6, 12, 24, 48, 96, 144, 192, 240, 312, 384 and 480 hours). Immediately after removing the agitator, the samples were centrifuged at 3500 rpm for fifteen minutes and then filtered

through a syringe filter with a 0.45 μm membrane. The amount of atrazine adsorbed by the biochar in each assay was calculated by [eq. (1)]:

$$\overline{q}(t) = \frac{V(C_0 - C(t))}{m} \tag{1}$$

Where:

V (L) - volume of atrazine solution;

C_0 (mg L^{-1}) - initial concentration of atrazine in the liquid phase;

$C_{(t)}$ (mg L^{-1}) - concentration of atrazine in the liquid phase at time t, and

m - mass (g) of the biochar (dry basis).

Adsorption isotherms

The assays were performed in batches to obtain the adsorption isotherms, considering the equilibrium time determined in the kinetic study. Five different concentrations of atrazine (5, 10, 15, 20 and 25 mg L^{-1}) were used, with triplicates at each concentration point. In glass tubes, 20 mg of biochar was weighed, followed by 10 mL of the atrazine solution. The system was maintained for 384 hours (equilibrium time) at a controlled temperature of 22 ± 0.5 °C and a rotation of 180 rpm. The samples were centrifuged at 3500 rpm after being removed from the shaker for a period of fifteen minutes. Then, they were filtered through a filter coupled to a syringe with a 0.45 μm membrane. After being filtered, the concentration of atrazine was determined, and the adsorbed amounts were calculated from [eq. (1)].

Mathematical models

The equilibrium data for atrazine adsorption on the biochars were evaluated by the Langmuir, Freundlich and BET models, all performed by Maple software.

The Langmuir mathematical model (Equation 2) is a theoretical equilibrium model, with a surface that is homogeneous and adsorption energy that is equal at all locations; there is no interaction between adsorbed molecules, and adsorption occurs in a monolayer.

$$q_{eq} = \frac{K_L q_{max} C_{eq}}{1 + K_L C_{eq}} \tag{2}$$

Where:

q_{max} (mg g^{-1}) - maximum adsorbed concentration;

K_L (L mg^{-1}) - Langmuir constant;

C_{eq} (mg L^{-1}) - adsorbate concentration in the liquid equilibrium phase, and

q_{eq} (mg g^{-1}) - amount of solute adsorbed per unit mass of adsorbent.

The Freundlich equation (Equation 3) was originally proposed as an empirical equation, and the model is based on heterogeneous surfaces, interactions between adsorbed molecules, and independent layers without interactions between them; thus, it is a multilayer system (Do, 1998).

$$q_{eq} = K_F C_{eq}^{\frac{1}{n}} \tag{3}$$

Where:

K_F (L mg^{-1}) - maximum adsorbent concentration;

n - Freundlich constant;

C_{eq} (mg L^{-1}) - adsorbate concentration in the liquid equilibrium phase, and

q_{eq} (mg g^{-1}) - concentration of the adsorbate on the adsorbent at equilibrium.

The BET model (Equation 4) was proposed as an extension of the Langmuir model, and it predicts that there is no limit to the number of layers that can connect to the surface material; adsorption occurs in several independent and immobile layers; and equilibrium is achieved in each layer individually (Do, 1998).

$$q_{eq} = \frac{q_m K_S C_e}{(1 - K_L C_{eq})(1 + (K_S - K_L) C_{eq})} \qquad (4)$$

Where:

q_m (mg g^{-1}) - amount of atrazine adsorbed on the surface of the biochar (in a monolayer);

K_S (L mg^{-1}) - monolayer adsorption equilibrium constant, and

K_L (L mg^{-1}) - adsorption equilibrium constant in multiple layers.

The intraparticle diffusion kinetic model, derived from Fick's Law, assumes that the diffusion of the liquid film surrounding the adsorbent is negligible and that intraparticle diffusion controls the stages of the adsorption process (Yang & Al-Duri, 2005). Fick's law was used to represent the intraparticle diffusion of atrazine in biochar produced from rice husk. Equation 5 is the result of applying the mass conservation law to atrazine with the assumption of a spherical shell as the control volume (Crank, 1979).

$$\frac{\partial}{\partial t} q(r,t) = \frac{D_{ef}}{r^2} \frac{\partial}{\partial r}\left(r^2 \frac{\partial}{\partial r} q(r,t)\right) \qquad (5)$$

Where:

D_{ef} (cm^2 h^{-1}) - effective diffusion coefficient of the atrazine molecule in each biochar.

The boundary conditions are described by eqs (6) and (7).

$$\frac{\partial}{\partial t} q(r = 0, t > 0) = 0 \qquad (6)$$

$$q(r = R, t > 0) = function(C(t)) \qquad (7)$$

Where:

R (cm) - radius of the biochar particles.

The Langmuir, Freundlich and BET models were applied to Equation 7, where the function (C (t)) is the mathematical representation for each equilibrium model (Equations 2-4).

Since this specific model considers the particles as spherical shells, an additional mathematical expression, presented in Equation 8, was used to determine the mean concentration of atrazine in the biochars of the rice husks ($\overline{q}$).

$$\overline{q}(t) = \frac{3}{R^3} \int_0^R r^2 q(r,t) dr \qquad (8)$$

The initial conditions for the solution of the model are given by eqs 9 to 11.

$$C(0) = C_0 \qquad (9)$$

$$\overline{q}(0) = 0 \qquad (10)$$

$$q(r,0) = 0 \qquad (11)$$

The line method was used to solve the intraparticle diffusion model (Equations 1-5), boundary and initial conditions (Equations 6-7 and 9-11) and auxiliary expression (Equation 8). Equation 5 was discretized in relation to the r coordinate. This procedure resulted in a system of ordinary differential equations and algebraic equations in time, which were solved by the Runge–Kutta–Fehlberg (RKF) method coded in Maple software (Monte Blanco et al., 2017).

Determination of the model and statistical parameters

The experimental equilibrium data provided the parameters for the Langmuir (q_{max}, K_L), Freundlich (K_F, 1 n^{-1}) and BET (q_m, K_S and K_L) isotherms, while the kinetic model parameters (D_{ef}) of all the investigated biochars were estimated from the adsorption kinetic data. The parameters D_{ef} were obtained from the kinetic model applied to the experimental kinetic data. The quality of the model fit was evaluated by the coefficient of determination (R^2) and the corrected Akaike information criterion (AICc) (Equation 13).

$$AIC = n\ln\left(\sum_{i=1}^{n} \frac{\left(\overline{q}_{exp,i} - \overline{q}_{mod,i}\right)^2}{n}\right) + 2(p+1) \qquad (12)$$

$$AICc = AIC + \frac{2(p+1)(p+2)}{n-p-2} \qquad (13)$$

Where:

$\overline{q}_{exp,i}$ and $\overline{q}_{mod,i}$ are the mean concentrations of atrazine in the solid phase of the experimental data and calculated by the kinetic models, respectively;

n - number of experimental observations, and

p - number of parameters of the fitted model.

RESULTS AND DISCUSSION

Characterization of biochars

Table 1 shows the results obtained for the physical and chemical properties of the biochars produced from rice husks. Regarding the specific surface area (SSA of the biochars), BCA400 showed a lower value than BCA700 (Table 1), with values of 4.167 and 98.43 m^2 g^{-1}, respectively. Tao et al. (2019) observed an increase in the SSA with increasing temperature. That is, the SSA values increased with increasing pyrolysis temperature, which is consistent with the results of Liu et al. (2019), who emphasized that the SSA is related to the raw material and the pyrolysis temperature used due to the escape of volatile substances, including cellulose, hemicellulose, and lignin, from the biomass (Ahmed et al., 2016).

Juliana Luconi, Mariana Sbizzaro, Cleuciane T. do Nascimento, et al.

TABLE 1. Physicochemical properties of the biochars.

	BCA400	BCA700
Specific surface area (m^2 g^{-1})	4.167	98.43
Micropore surface area (m^2 g^{-1})	4.976	163.6
Mean pore size (Å)	15.89	15.78
Total pore volume (cm^3 g^{-1})	0.005251	0.06489
Micropore volume (cm^3 g^{-1})	0.001768	0.05814

Based on the average pore size, both biochars produced from rice husks (BCA400 = 15.89 Å and BCA700 = 15.78 Å) can be classified as microporous materials (IUPAC, 1985). Even if classified as microporous, the presence of macro- and mesopores is possible. The total pore volume for BCA400 was lower than that observed for BCA700. In addition, the contribution of micropores to BCA700 (90%) was higher than that to BCA400 (47%). These values are associated with the pyrolysis temperature subjected to the production of the biochars, with a lower total volume of pores to the biochar at the lowest temperature.

The size of the atrazine molecule was estimated by the 3D visualization software MolView v2.4 to evaluate the adsorption of atrazine on the pores of the rice husk biochars, for which a longitudinal diameter (D_{long}) of 7.6 Å and diameter of projection (D_{pj}) of 7.3 Å were obtained. The average pore size and the microporous characteristics of the biochars indicate adsorption of the atrazine molecule may have occurred since the atrazine diameter was smaller than the pore size of the biochars studied. There is evidence that the maximum adsorption capacity is highly dependent on the volume of micropores, where pores larger than the atrazine diameter (7.1 Å) in the adsorbents are highly effective in removing atrazine (Yang et al., 2017).

From the analysis of the adsorption/desorption isotherm profile of N2 for BCA400 (Figure 1a), BCA400 was classified as a type II isotherm with H4-type hysteresis. Type II isotherms are related to nonporous or macroporous adsorbents. BCA400 had a low total pore volume and low SSA; therefore, it was a low or nonporous material. The hysteresis phenomenon was observed and classified as H4; however, the intensity of hysteresis was low (caused by the micropore fraction). In addition, the mean pressure of hysteresis (P/P0 <0.99) also suggests that the solid had a micromesopore in its structure (Thommes et al., 2015).
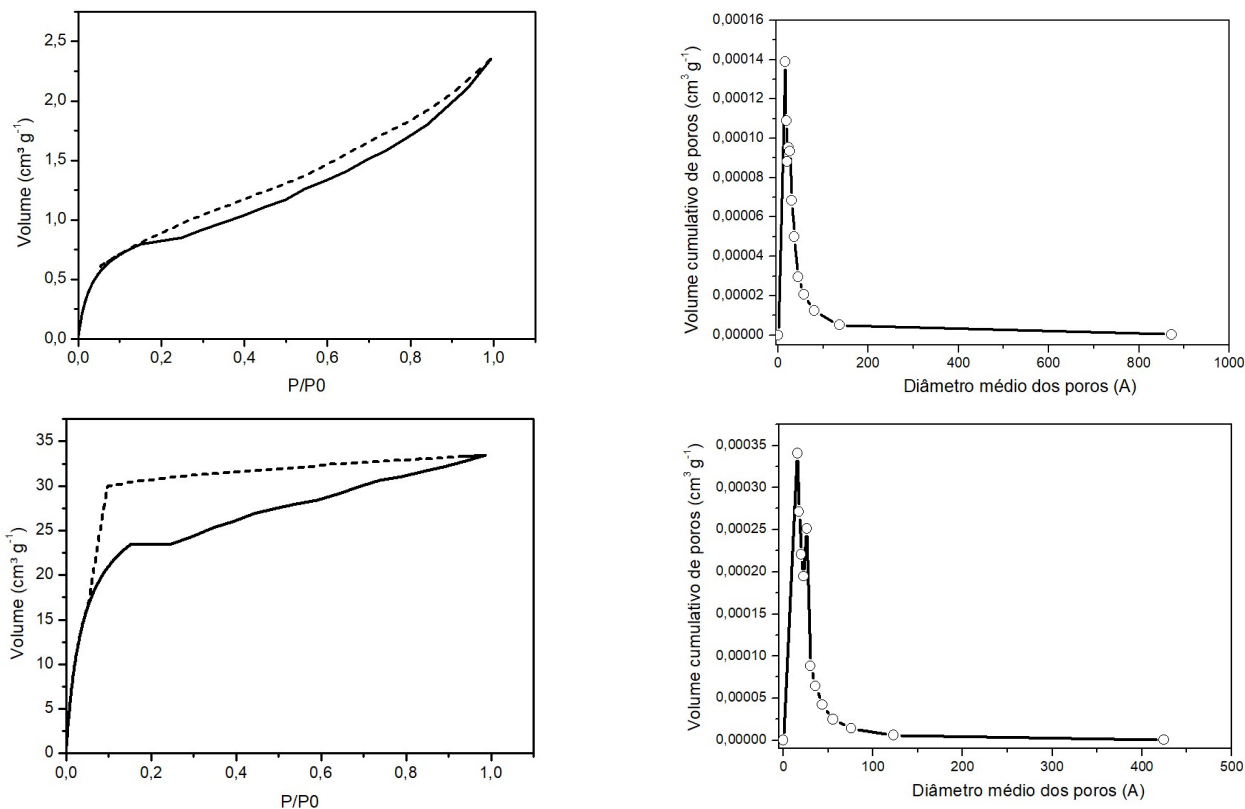
FIGURE 1. A) N2 adsorption-desorption isotherm for the rice husk BCA400 (adsorption; desorption); B) pore size distribution for rice husk BCA400; C) N2 adsorption-desorption isotherm for the rice husk BCA700 (adsorption; desorption); and D) pore size distribution for rice husk BCA700.

From Figure 1 (b), it is possible to observe that BCA400 has a significant portion of mesopores but also contains micropores. The textural parameters of BCA400 associated with the N2 isotherm profile confirmed the nonporous character of this biochar, however, with the contribution of micromesopores.

Based on the analysis of the adsorption/desorption isotherm profile of N2 for BCA700 (Figure 1c), this biochar was classified as a type IV isotherm with H4-type hysteresis.

Type IV isotherms are found in mesoporous materials. Although BCA700 was classified as having micropores, (Figure 1d) there was a significant portion of mesopores. The textural parameters of BCA700 associated with the N2 isotherm profile confirmed the predominance of micromesopores in the biochar, with a greater contribution of micropores (90%). H4 hysteresis is often found in micromesoporous activated carbons. The high number of micropores caused high hysteresis in the material. The mean

pressure of the hysteresis (P/P $_0$ <0.9880) also suggests that the solid had a micromesopore in its structure.

The set of micrographs shows the surface morphologies of the rice husk biochars. Both biochars exhibit irregular surface texture, with a higher incidence of micropores (less than 20 Å) (Figure 2a, 2b). The structures of BCA400 were not completely defined, according to

Rehraha et al. (2016), due to the persistence of organic matter in biochars produced at lower temperatures (Figure 2c). BCA700 showed better organization of the material, thus having better structural definitions. "Honeycombs" are beginning to form based on the different geometric formations and different porous spaces on the external surface (Figure 2d).
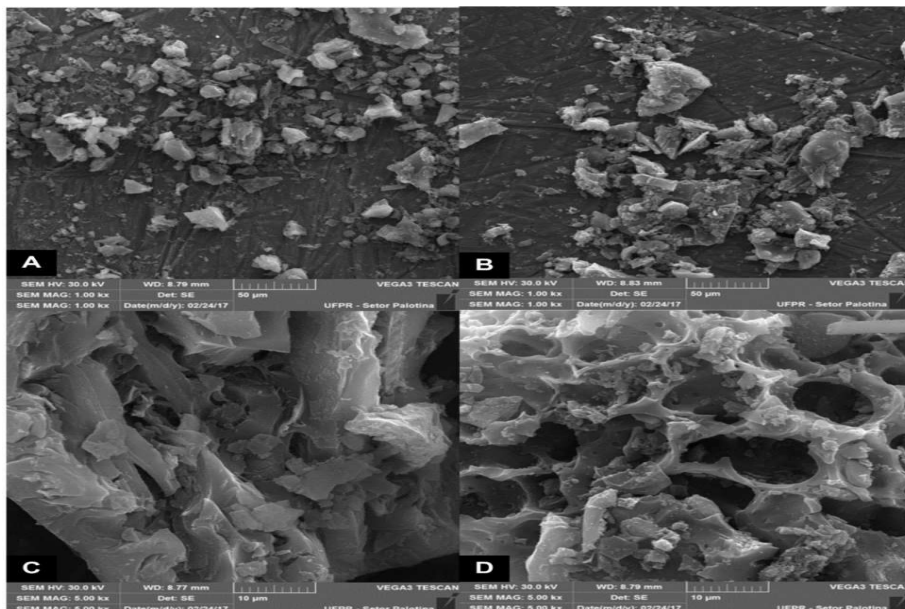
FIGURE 2. Scanning electron microscopy images A) BCA400, B) BCA700, C) enlarged image of BCA400, and D) enlarged image of BCA700.

The pore space increased with the increase in pyrolysis temperature due to the loss of volatile substances, such as cellulose and hemicellulose (Wang et al., 2017). These larger spaces on BCA700 cause this biochar to have a large SSA. Thus, the pyrolytic temperature played an important role in determining its adsorption properties (Yang et al., 2018; Tao et al., 2020).

Figure 3 shows the infrared spectroscopy analysis

for the biochars. The FTIR analysis showed significantly broad and extended bands in the region of 3700-3000 cm^{-1} for the two biochars. This region can be attributed to the stretching of the hydroxyl-OH functional groups. These bands were less pronounced in BCA700 than in BCA400 and indicated greater water loss occurred when the biochar was produced at a higher temperature (Yi et al., 2016).
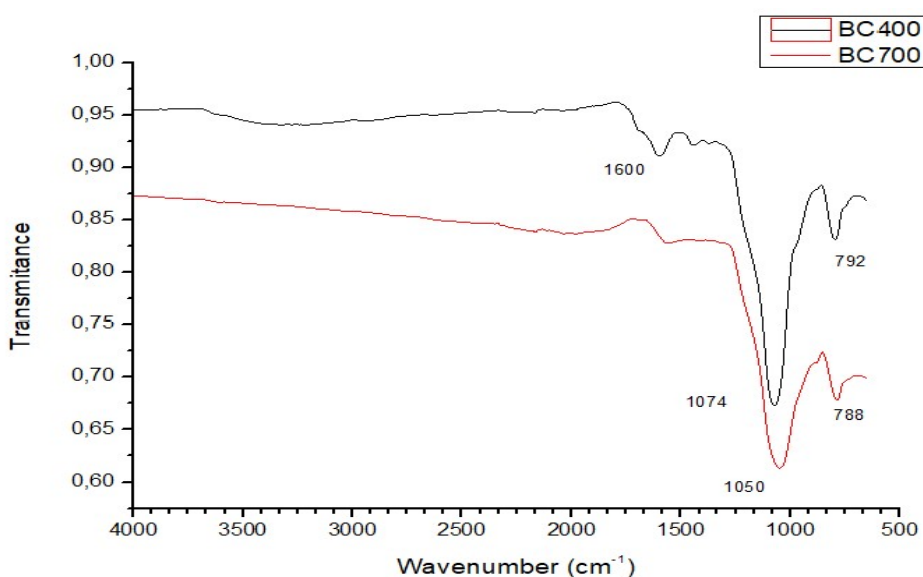
FIGURE 3. Results of FTIR spectroscopy for BCA400 and BCA700.

The BCA400 biochar had a significant peak at 1600 cm^{-1}, which is attributable to carboxylic groups (Zhao et al., 2018; Oliveira Ferreira et al., 2019). In a study of rice husk biochar, Kizito et al. (2015) found a peak at 1599 cm^{-1}, indicating high aromaticity. The most significant peaks observed were 1074 and 792 cm^{-1} in BCA400 and 1050 and 788 cm^{-1} in BCA700. Wave peaks below 1100 cm^{-1} are associated with groups containing cellulose, silicon (Mobarak et al. 2019; Hameed et al., 2020) and lignin (Kizito et al., 2015; Chen et al., 2019).

In general, the pyrolytic temperature significantly influenced the surface functional groups of the biochars, with a decrease in most bands at higher pyrolytic temperatures.

Mathematical models

Balance

The experimental adjustments to the isotherms of the Langmuir, BET and Freundlich models are shown in Figure 4. It was clear that the amount of atrazine adsorbed increased with increasing concentrations, showing a typical isotherm favorable for BCA400 and BCA700.

The final values of Q_{eq} were 1.03 mg g^{-1} for BCA400 and 1.85 mg g^{-1} for BCA700. Liu et al. (2015) studied the removal of atrazine by comparing several biochars derived from agricultural residues and observed Q_{eq} values ranging from 3.7 mg g^{-1} to 1.5 mg g^{-1}.
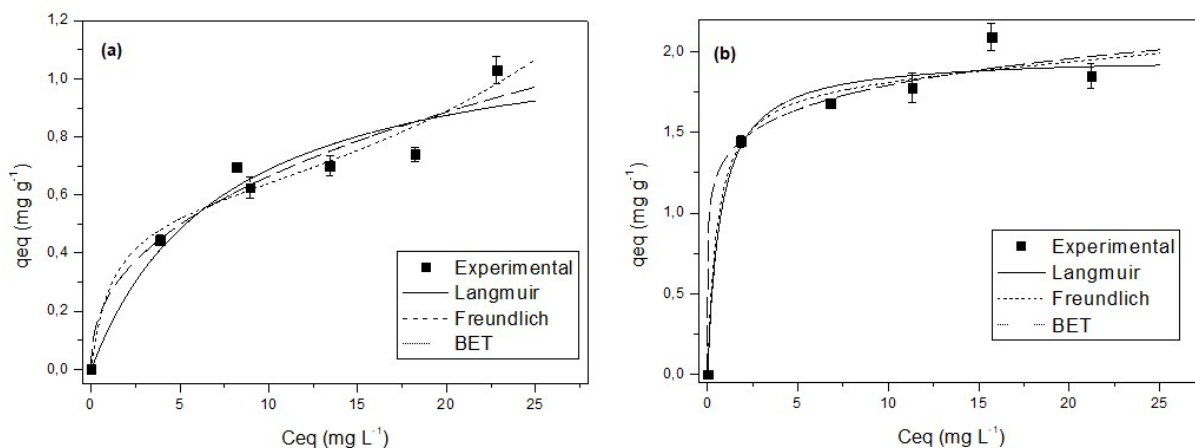
FIGURE 4. Experimental equilibrium data of atrazine adsorption in BCA400 (a) and BCA700 (b).

The estimated parameters of the model obtained from the adjustments to the experimental equilibrium data are shown in Table 2.

TABLE 2. Estimated parameter values of the isotherm models from the experimental data of atrazine adsorption on rice husk biochars - BCA400 and BCA700.

Isotherm Model	Parameters	BCA400	BCA700
Langmuir	q_{max} (mg g^{-1})	1.197	1.972
	K_L (L mg^{-1})	0.135	1.371
	R^2	0.9700	0.9890
	AICc	-19.70	-17.43
BET	q_{max} (mg g^{-1})	0.562	1.827
	K_S (L mg^{-1})	0.885	1.875
	K_L (L mg^{-1})	0.0193	0.0039
	R^2	0.9836	0.9897
	AICc	-8.14	11.87
Freundlich	K_f (mg g^{-1})(mg L^{-1})[1/n]	0.2551	1.339
	1/n	0.415	0.126
	R^2	0.9768	0.9904
	AICc	-21.39	-18.56

BCA700 had a greater capacity in the analyzed models. Based on its textural properties, the good adsorption capacity of BCA700 can be attributed to its higher SSA, greater total pore volume, pore size, and functional surface groups, which can facilitate the adsorption of atrazine in the adsorbent pore.

These results are similar to those found in a study by Gao et al. (2019), who observed higher atrazine adsorption capacity in biochar at 800 °C compared to at 300 °C. The adsorption capacity of biochar is influenced by the total pore volume and pyrolysis temperature; the higher the volume and temperature are, the greater the adsorption capacity (Zhao et al. 2013; Liu et al., 2015).

For the parameter K_L, which expresses affinity between the adsorbent and the adsorbate (Sheng et al., 2004), the values were higher for BCA700. Thus, it is concluded that the affinity between the adsorbent and atrazine is higher in biochar produced at a higher temperature. This conclusion indicates that in the adsorption process, these ions remain closely linked to the adsorption sites of the adsorbent.

The constant n is an empirical parameter related to the adsorption force of the adsorbent. When $1 \, n^{-1}$ is less than 0.5, substances are more easily adsorbed, while values greater than 2 indicate adsorption difficulty (Shi et al., 2014). The values of $1 \, n^{-1}$ for both biochars were lower than 0.5 (BCA400 = 0.415 and BCA700 = 0.126), and the results indicate that BCA700 had a higher affinity between biochar and atrazine. The parameter K_F is an approximate measure of the adsorption capacity of the adsorbent; the higher its value is, the greater the adsorption capacity (Lázaro et al., 2008). The K_F parameter also showed that BCA700 had a greater affinity for atrazine because its value at 1.339 was significantly higher than that of BCA400 at 0.2551.

When the values of R^2 approach 1, this is a strong indication that the proposed model fits the observed data. Thus, the values obtained for R^2 in Table 2 indicate the occurrence of mono- and multilayer adsorption of atrazine by the rice husk adsorbents since all models had satisfactory values of R^2, which were close to 1.

In addition, the use of the AICc is recommended when the number of samples/model parameters (n/p ratio) is less than 40, as was the case in this study. Lower AICc values indicate which model has the best fit, i.e., assumed to be the most appropriate to represent contaminant adsorption (Burnham & Anderson, 2004). The lowest AICc values found for both biochars were for the Freundlich isotherm, with values of -21.39 and -18.56 for BCA400 and BCA700, respectively.

Statistical parameters associated with graphical interpretation should be analyzed to determine which model is actually more consistent. The adsorption capacity, R^2, and AICc values were observed simultaneously, together with graphical interpretation. Good mathematical adjustments were observed in the Langmuir model for BCA400, suggesting adsorption in monolayers, and in the Freundlich model for BCA700, suggesting adsorption in multiple layers.

As the three analyzed isotherms can model the equilibrium data, atrazine adsorption in rice husk biochars is not a strict monolayer physical adsorption process, and some chemical interactions may be involved. Thus, to classify an adsorption system as favorable and the adsorbent as viable, knowledge about the adsorption kinetics is necessary. Therefore, experiments on the kinetic adsorption for atrazine on the rice husk biochars were performed, and the data obtained were analyzed by an intraparticle diffusion model to evaluate the mass transfer mechanism of the process.

Kinetics

The contact time between the adsorbents (BCA400 and BCA700) and the adsorbate (atrazine) plays an important role in the adsorption process. Figure 5 shows the experimental and simulated adsorption kinetics of the atrazine-biochar system for the two adsorbents. It was observed that atrazine was adsorbed more rapidly in the first 24 hours for both biochars, with 5% and 19% removal for BCA400 and BCA700, respectively.

The rate of atrazine removal depends on the particle size of the biochar since the smaller the particle size is, the less time the biochar needs to reach adsorption equilibrium. Zheng et al. (2010) indicated that in comparison to biochars with larger particle sizes, biochars with particle sizes less than 0.075 mm required a shorter time to reach equilibrium. After 24 hours, there was a slower adsorption phase, reaching equilibrium at 240 hours, with 14% removal of atrazine, for BCA400 and reaching equilibrium at 384 hours, with 42% for BCA700. These values are close to those found by Liu et al. (2015) and Zhao et al. (2013), who indicated a slow adsorption of atrazine in their study.

According to Liu et al. (2015), there are three steps in the adsorption process: (1) an instantaneous adsorption phase, (2) a subsequent slow adsorption phase, and (3) the equilibrium phase. Thus, this decrease in adsorption capacity over time can be attributed to the gradual blocking of micropores and mesopores by atrazine molecules (Vithanage et al., 2016).

Before reaching equilibrium, the adsorption of organic contaminants occurs gradually and is controlled by the intraparticle diffusion mechanism (Zhao et al. 2013). Previous studies on the kinetic behavior of contaminant adsorption on biochars showed that intraparticle diffusion is important in the adsorption process (Oliveira Ferreira et al., 2019). Therefore, the results of the morphological analysis are consistent with the identification of the mass transfer rate limitation.
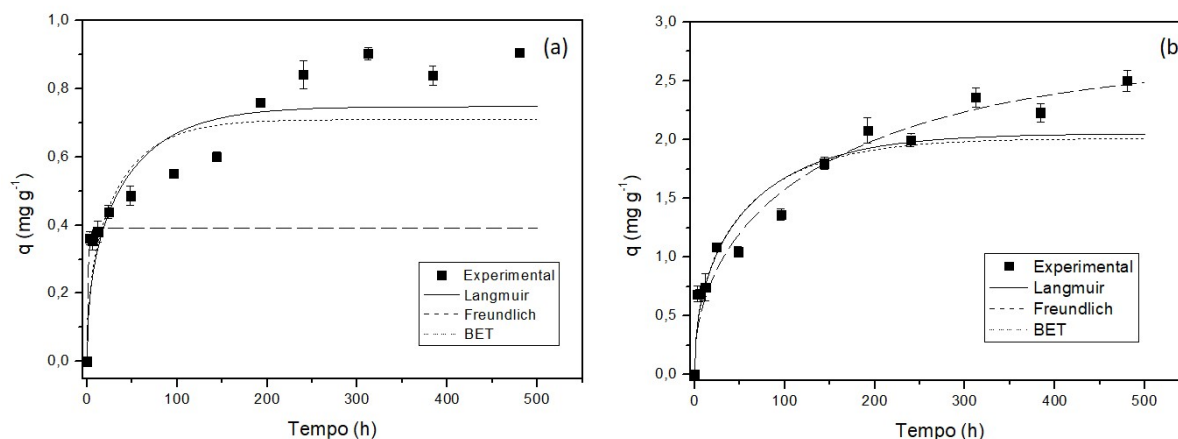
FIGURE 5. Kinetic data of atrazine adsorption in A) BCA400 and B) BCA700.

The intraparticle diffusion process is slow and probably involved the transport of atrazine to the pores of the biochar. Thus, the model was used to identify the rate limitation step in the adsorption process. When considering the molecular dimensions of atrazine in association with the textural properties of the biochars, the intraparticle diffusion mechanism was consistent.

Table 3 shows the kinetic parameters for the two rice husk biochars. The Langmuir, Freundlich, and BET models were applied to the intraparticle diffusion equations. The Freundlich model did not represent BCA400. Based on statistical parameters and graphical interpretation, the Langmuir model provided the best fit for BCA400, and the Freundlich model provided the best fit for BCA700.

TABLE 3. Values of the estimated parameters of the kinetic models from the experimental data of atrazine adsorption on rice husk biochar - BCA400 and BCA700.

Isotherm model applied to the kinetic model	Parameters	BCA400	BCA700
Langmuir	D_{ef} (cm^2 h^{-1})	2.61×10^{-8}	1.78×10^{-8}
	R^2	0.9307	0.9623
BET	D_{ef} (cm^2 h^{-1})	3.41×10^{-8}	1.91×10^{-8}
	R^2	0.9174	0.9591
Freundlich	D_{ef} (cm^2 h^{-1})	7.99×10^{-7}	5.59×10^{-9}
	R^2	0.6653	0.9851

The relatively high R^2 values of the intraparticle diffusion model indicate that the model successfully describes the adsorption kinetics mechanism. D_{ef} exhibited fluctuating behavior, with lower values for BCA700 than for BCA400. Despite the better properties of BCA700 compared to those of BCA400, the pore size of BCA400 was larger, possibly explaining the diffusivity of the atrazine molecule on BCA400, which was slightly higher than that on BCA700. This lower value may also have been associated with the higher volume of BCA700 micropores and thus lower resistance.

Analysis of the equilibrium and kinetics data showed that the Langmuir model was the most appropriate isotherm to represent the experimental data of BCA400; therefore, there were indications of adsorption in monolayers. The textural parameters showed that the biochars had small pore sizes and the arrangement of more than one layer of atrazine molecules on the biochar surfaces was highly likely. However, with respect to BCA700, the isotherm that best fit the experimental data was the Freundlich isotherm, indicating adsorption in multiple layers.

Environmental significance

Biochar has been widely used as an effective adsorbent for environmental remediation. It has the potential to remove both organic and inorganic contaminants due to its high specific surface area, high porosity, various functional surface groups, high cation exchange capacity, and carbon sequestration capacity (Liang et al., 2017).

This material has the potential to sequester carbon, improve soil physical quality, increase crop productivity, decrease nutrient leaching, reduce irrigation and fertilizer requirements, and serve as a contaminant adsorbent material (Tan et al., 2015; Zhang et al., 2015). al., 2015; Usman et al., 2016).

The production of biochar from agricultural waste is very beneficial with regard to waste management, as it has great potential to manage the flow of waste from animals and plants, thus reducing the contamination load to the environment that would occur if these wastes were not used.

The biomass used for biochar production includes crop residues, forest residues, animal residues, and animal manure (Ahmad et al., 2014).

CONCLUSIONS

The results indicated that the biochars produced from rice husks were efficient at removing the herbicide atrazine. However, the biochar produced at the highest pyrolysis temperature (BCA700) had a much higher maximum adsorption capacity than that (BCA400) produced at the lowest temperature. Thus, the increase in pyrolysis temperature had a positive effect on the production of biochar, corroborating the results of previous studies that show this same trend.

The Freundlich isotherm was able to describe the experimental equilibrium data for BCA700 well. The application of mathematical modeling to the experimental data obtained through simulation using a phenomenological model of intraparticle diffusion was useful for evaluating the mass transfer mechanism related to the process. It was found that intraparticle diffusion consistently described the kinetic data of atrazine adsorption on rice husk biochar. Thus, studying the characteristics of biochar associated with an investigation of the mass transfer mechanism is essential for evaluating the general adsorption mechanism.

The good atrazine adsorption capacity of rice husk biochar demonstrates the potential of this material in the removal of pesticides in aqueous media. Considering the management of agroenvironmental residues, the biochars produced from rice husks have potential applicability for pesticide removal by adsorption because in addition to being inexpensive materials, they were efficient at removing atrazine.

REFERENCES

Abdulrazzaq H, Jol H, Husni A, Abu-Bakr R (2014) Characterization and Stabilisation of Biochars Obtained from Empty Fruit Bunch, Wood, and Rice Husk. BioResources 9:2888-2898.

Ahmad M, Rajapaksha AU, Lim JE, Zhang M, Bolan N, Mohan D, Vithanage M, Lee SS, Ok YS (2014) Biochar as a sorbent for contaminant management in soil and water: A review. Chemosphere 99:19-23.

Ahmed MB, Zhou JL, Ngo HH, Guo W (2016) Insight into biochar properties and its cost analysis. Biomass and Bioenergy 84:76-86.

Budemberg ER (2013) Caracterização da sílica amorfa extraída da casca de arroz obtida por pré-hidrólise ácida e calcinação, e sua aplicação em borracha de estireno-butadieno (SBR). PhD Thesis, Universidade de São Paulo, Escola de Engenharia de Lorena.

Burnham KP, Anderson DR (2004) Multimodel inference: understanding AIC and BIC in model selection. Sociological Methods and Research 33:261-304.

Chen S, Qin C, Wang T, Chen F, Li X, Hou H, Zhou M (2019) Study on the adsorption of dyestuffs with different properties by sludge-rice husk biochar: Adsorption capacity, isotherm, kinetic, thermodynamics and mechanism. Journal of Molecular Liquids 285:62-74.

Crank J (1979) The Mathematics of diffusion. Oxford, Clarendon Press, Oxford.

de Oliveira Ferreira ME, Vaz BG, Borba CE, Alonso CG, Ostroski IC (2019) Modified activated carbon as a promising adsorbent for quinoline removal. Microporous and Mesoporous Materials 277:208-216.

Do DD (1998) Adsorption analysis: equilibria and kinetics. Series on chemical engineering 2. London, Imperial College Press.

Gao Y, Jiang Z, Li J, Xie W, Jiang Q, Bi M, Zhang Y (2019) A comparison of the characteristics and atrazine adsorption capacity of co-pyrolysed and mixed biochars generated from corn straw and sawdust. Environmental Research 172:561-568.

Hameed R, Lei C, Lin D (2020) Adsorption of organic contaminants on biochar colloids: effects of pyrolysis temperature and particle size. ESPR 27:18412-18422.

IUPAC - International Union of Pure and Applied Chemistry (1985) Reporting Physisorption Data for Gas/Solid Systems with Special reference to the Determination of Surface Area and Porosity. Pure Applied Chemistry 57:603-619.

Kizito S, Wu S, Kirui WK, Lei M, Lu Q, Bah H, Dong R (2015) Evaluation of slow pyrolyzed wood and rice husks biochar for adsorption of ammonium nitrogen from piggery manure anaerobic digestate slurry. Science of the Total Environment 505:102-111.

Lázaro DA, Mansur MB, Franca AS, Oliveira LS, Rocha SDF (2008) Performance of cold-pressed cake from Raphanus sativus (L.Var.) oilseeds, a solid residue from biodiesel production, as adsorbent for basic dyes. International Journal of Chemical Engineering 1:289-302.

Liang J, Yang Z, Tang L, Zeng G, Yu M, Li X, Wu H, Qian Y, Li X, Luo Y (2017) Changes in heavy metal mobility and availability from contaminated wetland soil remediated with combined biochar-compost. Chemosphere 181:281-288.

Lingamdinne LP, Roh H, Choi YL, Koduru, JR, Yang JK, Chang YY (2015) Influencing factors on sorption of TNT and RDX using rice husk biochar. Journal of Industrial and Engineering Chemistry 32:178-186.

Liu N, Charrua AB, Weng CH, Yuan X, Ding F (2015) Characterization of biochars derived from agriculture wastes and their adsorptive removal of atrazine from aqueous solution: A comparative study. Bioresource Technology 198:55-62.

Liu Y, Sohi SP, Jing F, Chen J (2019) Oxidative ageing induces change in the functionality of biochar and hydrochar: Mechanistic insights from sorption of atrazine. Environment Pollution 249:1002-1010.

Mobarak M, Mohamed EA, Selim AQ, Mohamed FM, Sellaoui L, Bonilla-Petriciolet A, Seliem MK (2019) Statistical physics modeling and interpretation of methyl orange adsorption on high–order mesoporous composite of MCM–48 silica with treated rice husk. Journal of Molecular Liquids 285:678-687.

Mohan D, Sarswat A, Ok YS, Pittman CU (2014) Organic and inorganic contaminants removal from water with biochar, a renewable, low cost and sustainable adsorbent – A critical review. Bioresource Technology. 160:191-202.

Monte Blanco SPD, Scheufele FB, Módenes AN, Espinoza-Quiñones FR, Marin P, Kroumov D, Borba CE (2017) Kinetic, equilibrium and thermodynamic phenomenological modeling of reactive dye adsorption onto polymeric adsorbent. Chemical Engineering Journal 307:466-475.

Rehraha D, Bansode RR, Hassanb O, Ahmedna M (2016) Physical-chemical characterization of biochars from solid municipal waste for use in soil amendment. Journal of Analytical and Applied Pyrolysis 118:42-53.

Ren X, Sun H, Wang F, Zhang P, Zhu H (2018) Effect of aging in field soil on biochar's properties and its sorption capacity. Environmental Pollution 242:1880-1886.

Sheng PX, Ting YP, Chen JP, Hong L (2004) Sorption of lead, copper, cadmium, zinc, and nickel by marine algal biomass: characterization of biosorptive capacity and investigation of mechanism. Journal of Colloid Interface Science 275(1):131-141.

Shi L, Zhang G, Wei D, Yan T, Xue X, Shi S, Wei Q (2014) Preparation and utilization of anaerobic granular sludge-based biochar for the adsorption of methylene blue from aqueous solutions. Journal of Molecular Liquids 198:334–340.

Suo F, You X, Ma Y, Li Y (2019) Rapid removal of triazine pesticides by P doped biochar and the adsorption mechanism. Chemosphere 235: 918-925.

Tan X, Liu Y, Zeng G, Wang X, Hu X, Gu Y, Yang Z (2015) Application of biochar for the removal of pollutants from aqueous solutions. Chemosphere 125:170-185.

Tao Y, Hu S, Han S, Shi H, Yang Y, Li H, Jiao Y, Zhang Q, Akindolie MS, Ji M, Chen Z, Zhang Y (2019) Efficient removal of atrazine by iron-modified biochar loaded Acinetobacter lwoffii DNS32. Science Total Environment 682:59-69.

Tao Y, Han S, Zhang Q, Yang Y, Shi H, Akindolie M S, Jiao Y, Qu J, Jiang Z, Han W, Zhang Y (2020) Application of biochar with functional microorganisms for enhanced atrazine removal and phosphorus utilization. Journal of Cleaner Production 257:120535.

Thommes M, Kaneko K, Neimark AV, Olivier JO, Rodriguez-Reinoso F, Rouquerol J, Sing KSW (2015) Physisorption of gases, with special reference to the evaluation of surface area and pore size distribution (IUPAC Technical Report). Pure and Applied Chemical 87(9). DOI: https://doi.org/10.1515/pac-2014-1117

Usman A, Sallam A, Zhang M, Vithanage M, Ahmad M, Al-Farraj A, Ok YS, Abduljabbar A, AlWaber M (2016) Sorption Process of Date Palm Biochar for Aqueous Cd (II) Removal: Efficiency and Mechanisms. Water Air Soil Pollution 227(12):1-16.

Vithanage M. Mayakaduwa SS, Herath I, Ok YS, Mohan D (2016) Kinetics, thermodynamics and mechanistic studies of carbofuran removal using biochars from tea waste and rice husks. Chemosphere 150: 781-789.

Wang X, Liu N, Liu Y, Jiang L, Zeng G, Tan X, Liu S, Yin Z, Tian S, Li J (2017) Adsorption removal of 17beta-Estradiol from water by rice straw-derived biochar with special attention to pyrolysis temperature and background chemistry. International Journal Environmental Research and Public Health 14 (10).

Yang F, Gao Y, Sun L, Zhang S, Li J, Zhang Y (2018). Effective sorption of atrazine by biochar colloids and residues derived from different pyrolysis temperatures. Environmental Science and Pollution Research 25:18528-18539.

Yang F, Sun L, Zhang, W, Zhang Y (2017) One-pot synthesis of porous carbon foam derived from corn straw: atrazine adsorption equilibrium and kinetics. Environmental Science: Nano 4:625-635.

Yang X, Al-Duri B (2005) Kinetic modeling of liquid-phase adsorption of reactive dyes on activated carbon. Journal Colloid Interface Science 287:25-34.

Yi S, Gao B, Sun Y, Wu J, Shi X, Wu B, Hu X (2016) Removal of levofloxacin from aqueous solution using rice-husk and woodchip biochars. Chemosphere 150:694-701.

Zhang J, Liu J, Liu R (2015) Effects os pyrolysis temperature and heating time on biochar obtained from the pyrolysis of straw and lingo-sulfonate. Bioresource Technology 176:288-291.

Zhang Y, Cao B, Zhao L, Sun L, Gao Y, Li J, Yang F (2018) Biochar-supported reduced graphene oxide composite for adsorption and coadsorption of atrazine and lead. Applied Surface Science 427:147-155.

Zhao L, Yang F, Jiang Q, Zhu M, Jiang Z, Tang Y, Zhang Y (2018) Characterization of modified biochars prepared at low pyrolysis temperature as an efficient adsorbent for atrazine removal. Environmental Science and Pollution Research International 25:1405-1417.

Zhao X, Ouyang W, Hao F, Lin C, Wang F, Han S, Geng X (2013) Properties comparison of biochars from corn straw with different pretreatment and sorption behaviour of atrazine. Bioresource Technology 147:338-344.

Zheng W, Guo M, Chow T, Bennett DN, Rajagopalan N (2010) Sorption properties of greenwaste biochar for two triazine pesticides. Journal Hazard Mater 181:121-126.